

The Roles of Acidity on Sono-Electrodeposition of Silver Nanoparticles

Kareem N. Abed¹, Ahmed Q. Abdullah¹, Abdulkareem M. A. Alsammarraie^{2*}

¹Physics Department, College of Science, University of Baghdad, Baghdad, Iraq

²Department of Chemistry, College of Science, University of Baghdad, Baghdad, Iraq

Email: *samuraee2000@hotmail.com

How to cite this paper: Abed, K.N., Abdullah, A.Q. and Alsammarraie, A.M.A. (2018) The Roles of Acidity on Sono-Electrodeposition of Silver Nanoparticles. *Materials Sciences and Applications*, 9, 671-678.

<https://doi.org/10.4236/msa.2018.98048>

Received: March 31, 2018

Accepted: July 3, 2018

Published: July 6, 2018

Copyright © 2018 by authors and Scientific Research Publishing Inc.

This work is licensed under the Creative Commons Attribution International

License (CC BY 4.0).

<http://creativecommons.org/licenses/by/4.0/>



Open Access

Abstract

The Ag NPs were produced by sonicating the electrochemical cell that the titanium horn serves as cathode and the anode was high purity silver foil, while the electrolyte in all experiments was (0.2 g Ag₂SO₄ in 250 ml deionized water), the pH was varied between 2 to 8 using sulfuric acid and sodium bicarbonate diluted solutions, the current density was maintained at 5mA/cm². The quality of the products was extensively examined using: SEM, TEM, AFM, XRD, UV-visible and EDX techniques. The results reflected a clear fact that the more acidic electrolyte (lower pH value) has produced distorted spherical larger AgNPs, with a narrow particles size distribution, while decreasing the acidity (higher pH value) led to smaller particle size, and wider size distribution spectrum.

Keywords

Silver Sulfate, Silver Nanoparticles, Sonoelectrodeposition, AFM

1. Introduction

Sonoelectrochemistry is the coupling of ultrasonic vibration to an electrochemical system. The term “sonochemistry” appeared at 1990 [1]. Recently there is a growing interest of the application of the sonochemistry in the preparation of nanopowders [2] [3] due to it is environmental friendly and cost effectiveness method compared to most of other methods including radiation, thermal decomposition, and vapor deposition, reduction in microemulsions and chemical reduction [4]. Ultrasound has been applied in the fields of electroplating, electroorganic synthesis, electropolymerisation, electroanalytical chemistry and for the electrochemical production of nanoparticles [5]. Sonochemical formation of nanoscale metals was accomplished by applying an electric cur-

rent pulse for electrodeposition, followed by a burst of ultrasonic energy that removes the particles from the son electrode [6]. The propagation of pressure waves in a fluid causes the formation of cavitation bubbles. At low irradiation intensity, these bubbles oscillate none linearly in the acoustic field. Above a threshold, called the transient cavitation threshold, the number of bubbles increases intensely. The collapse of these bubbles, described as an implosion in the hot-spot theory, or described as a fragmentation in the electrical theory, is at the origin of extreme local conditions: high temperature and high pressure following the hot-spot theory, high electrical fields following the electrical theory [7] [8]. When the irradiation intensity is higher than the threshold intensity, the collapse of the bubbles is also associated with shock waves and microstreaming. Mechanical effects including erosion of solids, fragmentation of solid particles in suspension and emulsification of non-miscible liquids can occur. Under the influence of these extreme local conditions and also of these mechanical effects, sonochemistry takes place. Sonochemistry, which is thus defined as chemistry induced by sound and ultrasound, is a fast developing field. It is well know that the final application highly depends on the particle size, in this work the particle size of Ag NPs was tuned by variation of the pH of the Ag_2SO_4 electrolyte.

2. Experimental

Figure 1 show the experimental set-up used. In these experiments titanium probe (20 kHz) acts both as a cathode and an ultrasound emitter. The electroactive part of the sonoelectrode is the planar circular surface at the bottom of the horn and the immersed cylindrical part into the electrolyte is covered by an isolating plastic jacket.

The ultrasound probe is connected to a power supply using a pulse driver. The system used the simplest configuration of a two-electrode cell, where the silver sheet used as anode. Before each experiment, the titanium sonoelectrode have been polished [9]. The electrochemical processes were performed at (20°C), the temperature of the electrolyte maintained to within $\pm 1^\circ\text{C}$ with cooling and

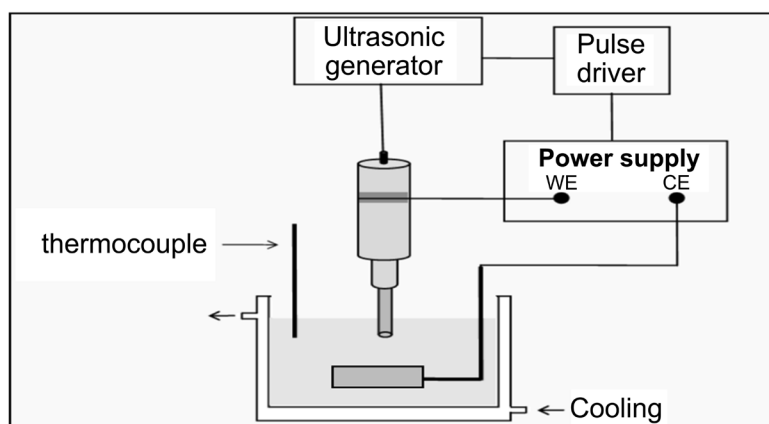


Figure 1. Sonoelectrochemistry set-up used in the production of nanopowders (WE working, and CE counter electrode).

heating water bath circulator. The distance between the anode and cathode was (30 mm). The working time of 1min was chosen, the electrolyte was (0.2 gm Ag_2SO_4 , from Nanjing Chemical Reagent Co. in 250 ml DI) and some drops of H_2SO_4 , 30 W/cm^2 ultrasound intensity and varying of pH value (2, 4, and 8). The silver foil was immersed in solution and using ultrasonic to obtaining silver nanoparticles. The produced AgNPs washed with distilled water and collected by Millipore nanofilter paper the characterized by atomic force microscopy (AFM), UV-visible spectra (UV-vis), Transmission electron microscopy (TEM) and X-ray diffraction (XRD) techniques.

The electroactive part of the sonoelectrode is the planar circular surface with an area of 7 cm^2 at the bottom of the horn. The immersed cylindrical part is covered by an isolating plastic jacket. A silver sheet ($2.0\text{ cm} \times 2.0\text{ cm}$) is used as a counter electrode.

3. Results and Discussion

SEM images in **Figure 2**, AFM images in **Figure 3**, and TEM images in **Figure 4** reflected the effect of the electrolyte acidity (pH) on the morphologies of the Ag NPs produced at current density of ($5\text{ mA}/\text{cm}^2$). These SEM and AFM images

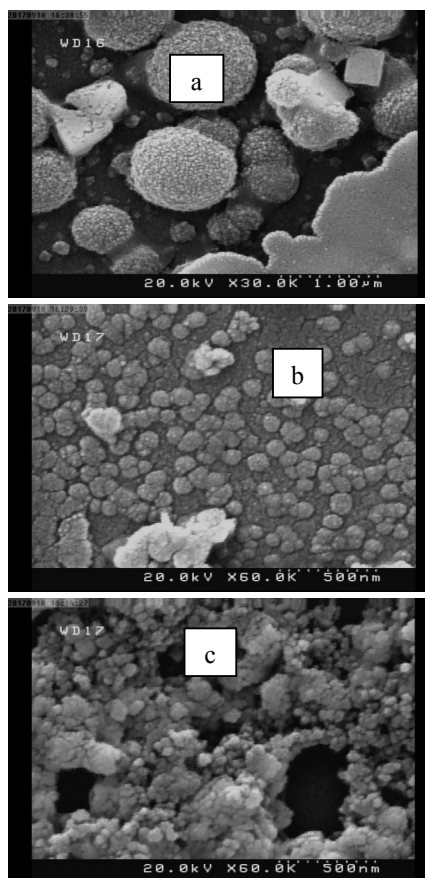


Figure 2. SEM images of Ag NPs produced by electrochemical sonication of Ag_2SO_4 electrolyte; (a) pH2; (b) pH5, and (c) pH8, all at $5\text{ mA}/\text{cm}^2$ for 1min with sonication power density of $30\text{ W}/\text{cm}^2$.

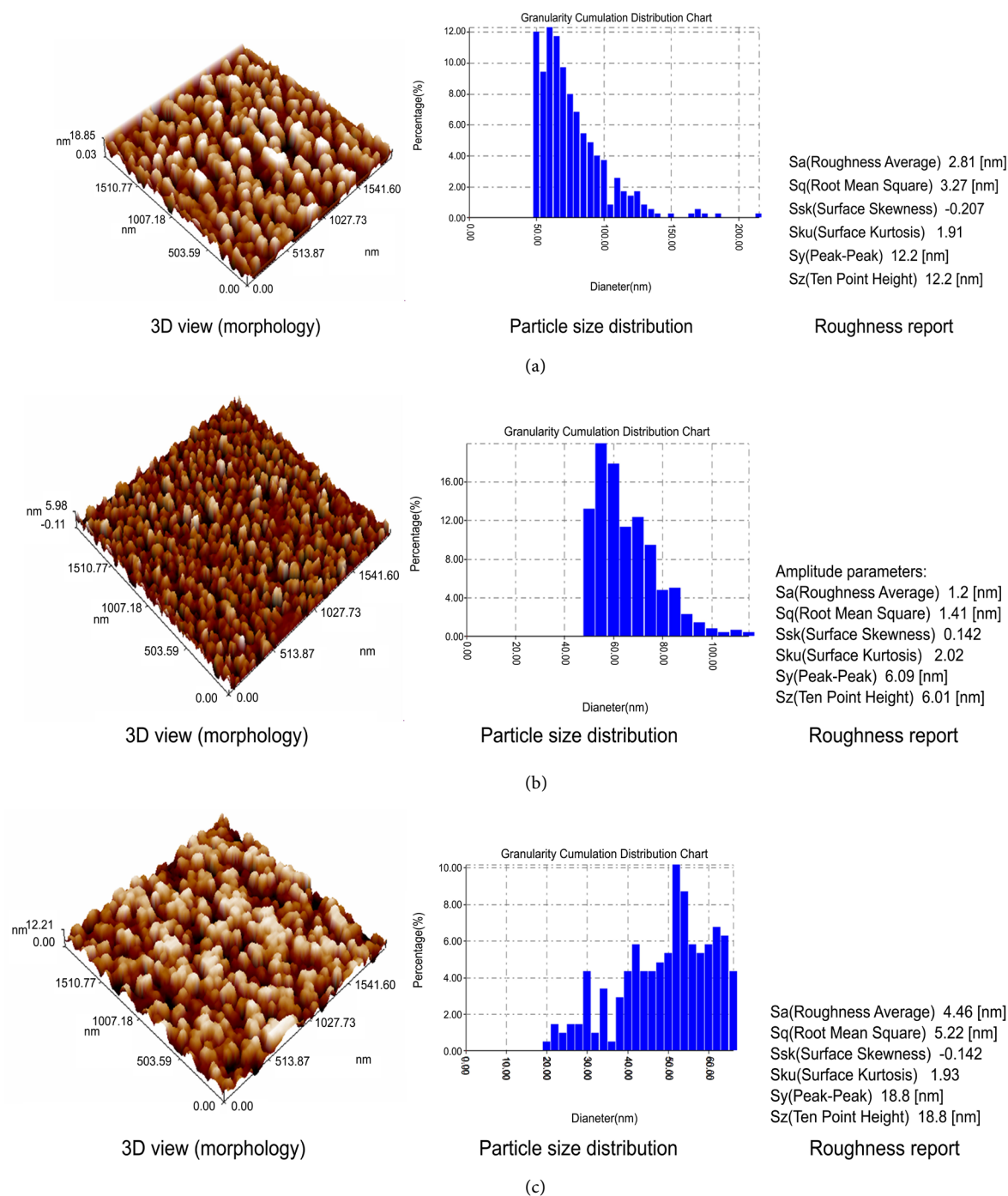


Figure 3. AFM images (3D, particles size distribution, and roughness reports) of Ag NPs produced by electrochemical sonication of Ag_2SO_4 electrolyte; (a) pH2; (b) pH5, and (c) pH8, all at 5 mA/cm^2 for 1min with sonication power density of 30 w/cm^2 .

reflected a clear fact that the more acidic electrolyte (lower pH value) have produced distorted spherical larger AgNPs (around 73 nm), with a narrow particles size distribution, while decreasing the acidity (higher pH value) led to smaller particle size (63 nm at pH5, and 48 nm at pH8), and wider size distribution spectrum. This manner may attributed to the lower repulsing forces between

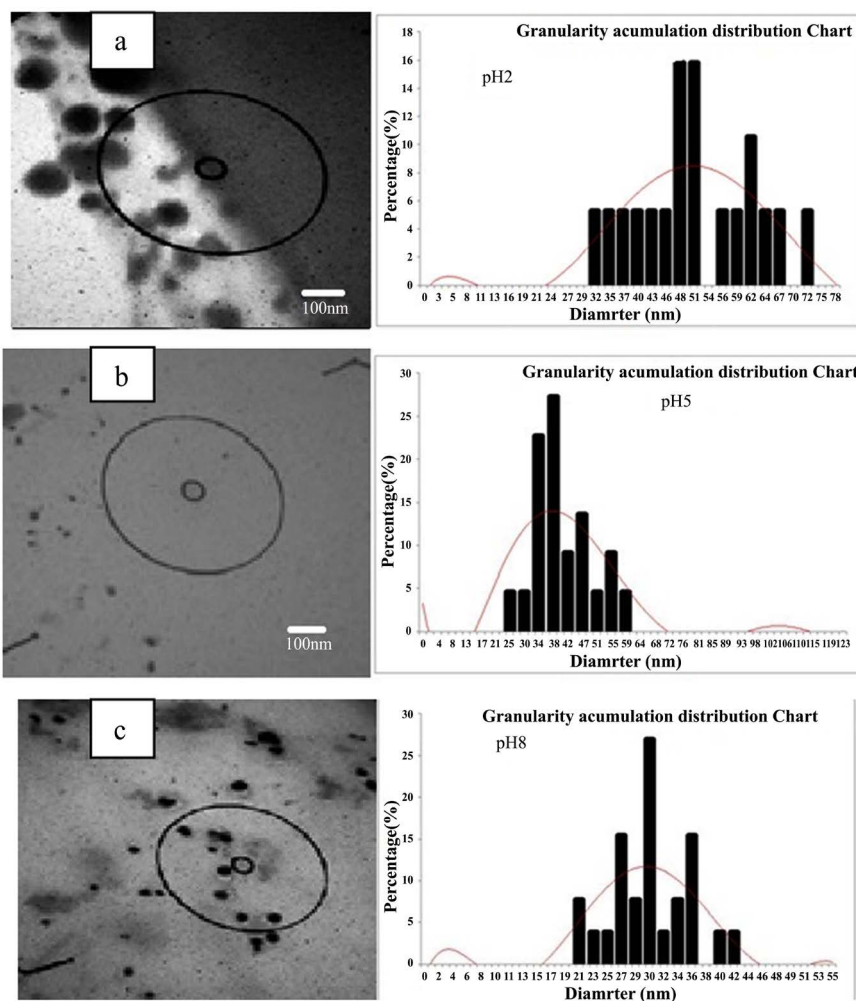


Figure 4. TEM images with granularity distribution of Ag NPs produced by electrochemical sonication of Ag_2SO_4 electrolyte; (a) pH2; (b) pH5; and (c) pH8, all at 5 mA/cm^2 for 1min with sonication power density of 30 W/cm^2 .

partially positive charged Ag particles because of the more numbers of free cations in the more acidic electrolyte [9].

The decreasing of the particle size follows the order: pH2 (73 nm) > pH5 (63 nm) > pH8 (48 nm).

The particle surface roughness (SR) according to the AFM analyses shows unorganized manner, the lowest (SR) was recorded at pH5 (1.2 nm) then at pH8 (2.8 nm), the higher value of (SR) was at pH2 (4.46 nm).

Figure 5 shows UV-Visible absorption spectrum of the aqueous solution of the produced Ag NPs at different pH values, the peak at 400 nm is a specific peak of Ag-NPs, and can therefore confirm the formation of NPs in the solution due to the surface Plasmon resonance (SPR) of Ag NPs, the smaller size is, the broader the absorption band will be [10]. By increasing the pH value the absorbance peaks shift to higher wavelength (red shift) meaning lower energies, the absorbance vs wavelength has a red shift for smaller particles.

Figure 6 represent a typical XRD pattern of the produced silver nanoparticles

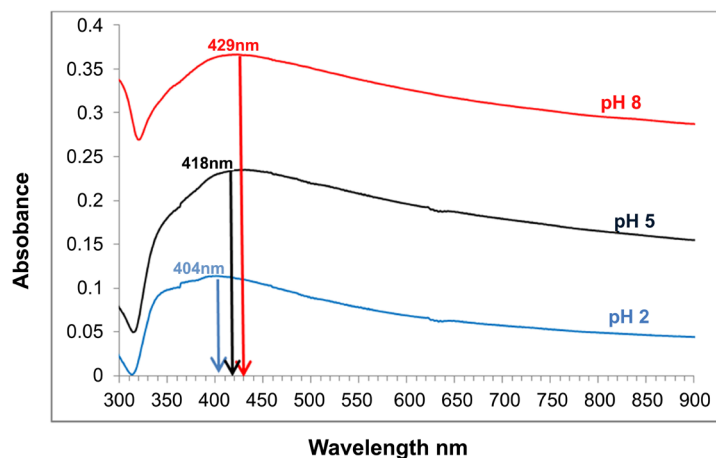


Figure 5. UV-VIS spectrums for AgNPs synthesized by sonoelectrochemical of Ag_2SO_4 electrolyte at different pH value.

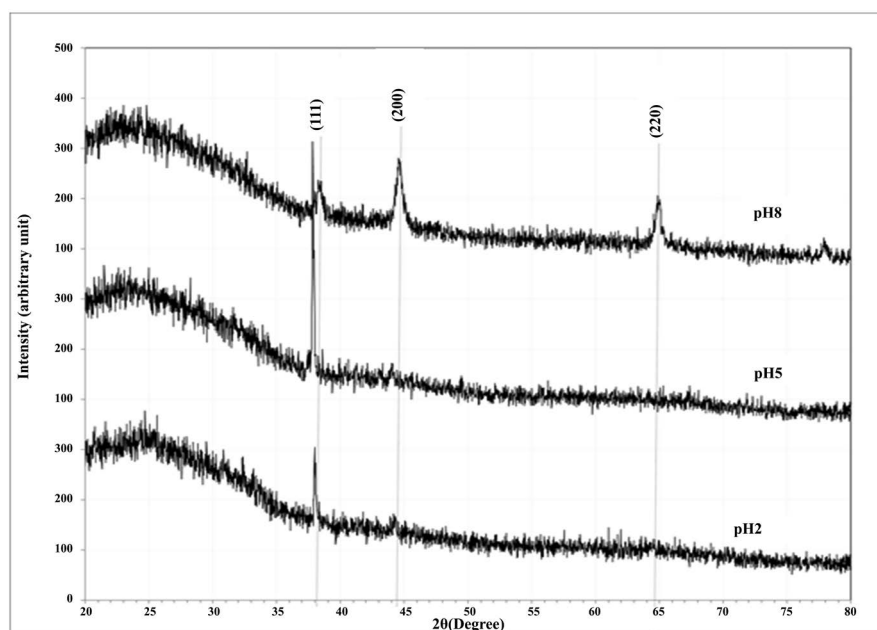


Figure 6. XRD spectrums of the Ag NPs synthesized by sonoelectrochemical of Ag_2SO_4 electrolyte at different pH value.

shows the presence of the diffraction peaks located at 38.35° , 44.58° and 64.8729° corresponding to (111), (200) and (220) planes and identical with face centered cubic (fcc) structure (Card No. 96-901-3047) [11]. The peaks being broad, *i.e.* the crystalline size decrease, with decreasing electrolyte acidity (higher pH) as shown in **Table 1**.

By comparing the grain size deduced from SEM and AFM images, with the crystallite size calculated from XRD spectrums using, Sheerer equation, the number of crystal in grain can be represented as the ratio between these two values [12], and the results are as follow: at pH2 = $73/37.7 = 2$, at pH5 = $63/16.1 = 4$, and at pH8 = $48/13.2 = 3.63$.

Table 1. XRD parameters of the Ag NPs synthesized by sonoelectrochemical method at different pH values. (a) pH2; (b) pH5; (c) pH8.

pH	2θ (Deg.)	FWHM (Deg.)	d _{hkl} Exp. (Å)	Crystallite Size (nm)	d _{hkl} Std.(Å)	hkl	card No.
2	37.9746	0.2230	2.3675	37.7	2.3723	(111)	96-901-3047
	44.1780	0.3559	2.0484	24.1	2.0545	(200)	96-901-3047
5	37.8220	0.2990	2.3767	28.1	2.3723	(111)	96-901-3047
	44.0508	0.5339	2.0540	16.1	2.0545	(200)	96-901-3047
	38.3559	0.6356	2.3449	13.2	2.3723	(111)	96-901-3047
8	44.5847	0.5339	2.0307	16.1	2.0545	(200)	96-901-3047
	64.8729	0.5593	1.4362	16.8	1.4528	(220)	96-901-3047

4. Conclusion

Sono-electrodeposition of AgNPs was succeeded using Ag₂SO₄ electrolyte, decreasing the acidity of the electrolyte (higher pH) in the range pH2 to 8 produced lower particle size of AgNPs.

References

- [1] Mason, T.J. and Lorimer, J.P. (2002) *Applied Sonochemistry: The Uses of Power Ultrasound in Chemistry and Processing*. Willey-VCH, Weinheim.
- [2] Sáez, V. and Mason, T.J. (2009) Sonoelectrochemical Synthesis of Nanoparticles. *Molecules*, **14**, 4284-4299. <https://doi.org/10.3390/molecules14104284>
- [3] Aqil, A., Serwas, H., Delplancke, J.L., Jerome, R., Jerome, C. and Canet, L. (2008) Preparation of Stable Suspensions of Gold Nanoparticles in Water by Sonoelectrochemistry. *Ultrasonics Sonochemistry*, **15**, 1055-1061. <https://doi.org/10.1016/j.ultsonch.2008.04.004>
- [4] Zin, V., Pollet, B.G. and Dabala, M. (2009) Sonoelectrochemical (20 kHz) Production of Platinum Nanoparticles from Aqueous Solution. *Electrochimica Acta*, **54**, 7201-7206. <https://doi.org/10.1016/j.electacta.2009.07.001>
- [5] Haas, I., Shanmugam, S. and Gedanken, A. (2006) Pulsed Sonoelectrochemical Synthesis of Size-Controlled Copper Nanoparticles Stabilized by Poly(*N*-Vinylpyrrolidone). *Journal of Physical Chemistry B*, **110**, 16947-16952. <https://doi.org/10.1021/jp064216k>
- [6] Atobe, M., Ishikawa, K., Asami, R. and Fuchigami, T. (2009) Size-Controlled Synthesis of Conducting Polymer Microspheres by Pulsed Sonoelectrochemical Polymerization. *Angewandte Chemie International Edition*, **48**, 6069-6072. <https://doi.org/10.1002/anie.200902062>
- [7] Zhu, J.-J., Qiu, Q.-F., Wang, H., Zhang, J.-R., Zhu, J.-M. and Chen, Z.-Q. (2002) Synthesis of Silver Nanowires by a Sonoelectrochemical Method. *Inorganic Chemistry Communications*, **5**, 242-244. [https://doi.org/10.1016/S1387-7003\(02\)00351-9](https://doi.org/10.1016/S1387-7003(02)00351-9)
- [8] Reisse, J., Francois, H., Vandercammen, J., Fabre, O., Kirsch-de Mesmaeker, A., Maerschalk, C. and Delplancke, J.-L. (1994) Sonoelectrochemistry in Aqueous Electrolyte: A New Type of Sonoelectroreactor. *Electrochimica Acta*, **39**, 37-39. [https://doi.org/10.1016/0013-4686\(94\)85008-9](https://doi.org/10.1016/0013-4686(94)85008-9)
- [9] Qin, X., Miao, Z., Fang, Y., Zhang, D., Ma, J., Zhang, L., Chen, Q. and Shao, X. (2012) Preparation of Dendritic Nanostructures of Silver and Their Characterization for Electroreduction. *Langmuir*, **28**, 5218-5226.

<https://doi.org/10.1021/la300311v>

- [10] Kumar, D., Bhui, H.B., Sarkar, P., Prasad, G., Sahoo, S.P. De, and Misra, A. (2009) Synthesis and UV-vis Spectroscopic Study of Silver Nanoparticles in Aqueous SDS Solution. *Journal of Molecular Liquids*, **145**, 33-37.
<https://doi.org/10.1016/j.molliq.2008.11.014>
- [11] MamtaBaunthiyal, K. and Singh, A. (2016) Characterization of silver Nanoparticles Synthesized Using *Urticadioica* Linn. Leaves and Their Synergistic Effects with Antibiotics. *Journal of Radiation Research and Applied Sciences*, **9**, 217-227.
<https://doi.org/10.1016/j.jrras.2015.10.002>
- [12] John, R. and Florence, S. (2010) Optical Structural and Morphological Studies of Bean-Like ZnS Nanostructures by Aqueous Chemical Method. *Chalcogenide Letters*, **7**, 269-273.